

VISCOUS-INVISCID INTERACTION FOR THE SOLUTION OF THE FLOW ABOUT AIRFOILS

Paulo Vatauvuk

Faculdade de Engenharia Civil, Arquitetura e Urbanismo, UNICAMP, Cx. Postal 6021, CEP 13083-852, Campinas, SP, Brasil.
pvatauvuk@fec.unicamp.br

Márcio Teixeira Mendonça

Instituto de Aeronáutica e Espaço, CTA, Pç Mal. Eduardo Gomes, 50, CEP 12228-904, São José dos Campos, SP, Brasil
Marcio_tm@yahoo.com

João Luiz F. Azevedo

Instituto de Aeronáutica e Espaço, CTA, Pç Mal. Eduardo Gomes, 50, CEP 12228-904, São José dos Campos, SP, Brasil
azevedo@iae.cta.br

Abstract. *Viscous-inviscid iteration is a technique for the analysis of flows that although not being as precise as a complete Navier-Stokes solution allows very small computational times and that makes it an ideal tool for preliminary or optimization studies. This work reports the coupling of an Euler solver with a differential boundary layer code, using the Cebeci-Smith turbulence model. Results are presented for the RAE 2822 airfoil in transonic and in subsonic flow with a high angle of attack. The results show that the coupling methodology is adequate and that convergence was obtained in critical conditions like the presence of shocks and separation. In the transonic flow, there is some disagreement with the experimental results for the pressure coefficient, previously published work indicate that this is probably due to the use of a coarse mesh.*

Keywords: *Aerodynamics, Viscous-inviscid iteration, Boundary-layer, Euler flow.*

1. Introduction

The importance of computational fluid dynamics (CFD) as a tool for the study of aerodynamic shapes has grown steadily in the last decades. At present the main focus of the applications is the solution of the Reynolds averaged Navier-Stokes (RANS) equations, with a suitable turbulence model. Some time ago, when the computational power was more limited, one of the most important tools was the solution of the inviscid flow using an Euler or a full-potential formulation. This solution requires much less computational resources because the mesh doesn't need to be so refined near the walls as in the complete Navier-Stokes formulation, and because the viscous terms in the equations tend to increase the number of iterations for convergence. The disadvantage of using an inviscid flow formulation alone is that the results become unrealistic when the viscosity has an important effect in the flow, like for instance in the calculation of shear. To improve the results, the inviscid flow may be solved coupled to a boundary layer solver, a technique called viscous-inviscid interaction (VII). Normally the solution of the boundary layer increases only a small percentage in the computational time so VII remains much more fast than a RANS solution. Lock and Williams (1987) cite a reduction of up to 40 times in CPU time using VII compared to RANS. So this technique is very useful in preliminary and optimization studies where a large number of shapes must be evaluated and a small error can be accepted.

The viscous-inviscid interaction involves coupling of an inviscid solver that uses either an Euler or a full-potential formulation to a boundary layer code that may be based in either the differential or the integral formulation of the boundary layer. The coupling of the inviscid and viscous flows is not simple because the inviscid flow will supply the external flow boundary condition for the solution of the boundary layer. On the other hand, the boundary layer will influence the inviscid flow, since the presence of the boundary layer will tend to deviate the streamlines away from the surface, like if the thickness of the airfoil was increased by the presence of the boundary layer. This influence can be taken into account in two ways:

a) Changing the geometry of the airfoil so as to include the displacement thickness of the boundary layer in the thickness of the airfoil.

b) Including, in the boundary conditions of the inviscid flow, a transpiration velocity, normal to the surface of the airfoil, which will produce the same deviation of the streamlines as the boundary layer. In this case, the transpiration velocity, v_n , will be given by:

$$v_n = \frac{1}{\rho_e} \frac{\partial(\rho_e u_e \delta^*)}{\partial s} \quad (1)$$

In the above equation, u_e is the speed outside the boundary layer, ρ_e is the specific mass outside the boundary layer, s is the longitudinal arc length coordinate, and δ^* is the displacement thickness that is defined as:

$$\delta^* = \int_0^{y_1} \left(1 - \frac{\rho u}{\rho_e u_e} \right) dy \quad (2)$$

Where, y is the coordinate normal to the wall and y_1 is the y coordinate of a point just outside the boundary layer. For more details see Anderson (1991).

The majority of the works with VII are made using the transpiration velocity method. The reason for this is that the other alternative, changing the geometry of the airfoil, is difficult to put into practice, because of the necessity to re-mesh the flow domain.

There are also many coupling methodologies cited in the literature, see for instance Anderson (1984) and Lock and Williams (1987). The first coupling methodology used was the direct one. In this methodology some inviscid iterations are done, then the boundary layer is calculated with the external velocity supplied by last inviscid iteration. After that the transpiration velocities are calculated and then new inviscid iterations are done. Then the boundary layer is calculated again and this process is repeated until convergence. This methodology is good for flows without separation, but when the boundary layer separates this method diverges. To obtain convergence the inverse method was developed. In this method, the boundary layer is calculated in the inverse mode, instead of using the external velocity as a boundary condition, the external velocity is calculated so as to match supplied values of shear or displacement thickness. This technique converges for separated flows, but don't converge in flows without separation. To obtain convergence with less iterations other techniques were devised, the most important being the semi-inverse and the quasi-simultaneous coupling. The objective of this work is to report the coupling of two preexisting codes, an Euler solver and a boundary layer solver, so as to obtain the viscous-inviscid iteration, the coupling methodology is a variation of the inverse method as described in item 2.3.

2. Methodology

In this section the formulation and the numerical methods used in the components of the viscous-inviscid interaction are described.

The Euler solver used was basically the one described in Scalabrin (2002). This solver uses the finite volume method and allows the solution of compressible flows with the Euler or full Navier-Stokes formulation. It uses an unstructured three-dimensional mesh, composed of elements of mixed type. In spite of other options available in the code, it was used, in essence, the scheme proposed by Jameson, Schmidt and Turkel (1981), with a fourth order Runge-Kutta integration in time, a centered scheme for spatial discretization and an artificial dissipation term given by the sum of a Laplacian and a bi-harmonic operator.

The boundary layer code uses a Keller box scheme to solve the two-dimensional compressible boundary layer as described in Cebeci (1999), but, instead of solving the energy equation, the temperature in the boundary layer is evaluated by the Crocco equation (see Schlichting, 1979). The turbulence model used was the one of Cebeci and Smith, which is a two-layer model in which the inner layer is calculated with the mixing length hypothesis and the external layer is calculated with an expression similar to the equation of Clauser for the defect layer. For more details on the turbulence model see Cebeci (1999). The solver uses the FLARE approximation (Cebeci, 1999), which consists in neglecting the convective term when the flow is separated, and so maintaining the parabolic character of the equations, and allowing a solution being obtained with a boundary layer code.

The coupling method used in this work is a variation of the inverse method, (see Cebeci, Bradshaw and Whitelaw, 1981). This method can be described as:

- a) First some inviscid iterations are made considering zero transpiration.
- b) Then the boundary layer is solved in inverse mode so as to minimize the following expression:

$$\left(u_e^b - u_e^i \right)^2 - \left(v_n^b - v_n^i \right)^2 = \min \quad (3)$$

Where u_e^i is the external velocity calculated by the inviscid code, v_n^i is the last transpiration velocity used as entry data for the inviscid flow calculation, u_e^b and v_n^b are the corresponding new values of the external velocities and transpirations from the inverse boundary calculation.

c) In order to improve the convergence of the iterative process the values of u_e^b and v_n^b are under-relaxed by the following expressions:

$$\bar{v}_n^b = p v_n^b + (1 - p) v_n^i \quad (4)$$

$$\bar{u}_e^b = p u_e^b + (1-p) u_e^i \quad (5)$$

In the above expressions p is the relaxation factor and \bar{v}_n^b and \bar{u}_e^b are the new values of the transpiration and external boundary layer velocities.

d) Then new inviscid iterations are performed with the new transpiration velocity \bar{v}_n^b . If convergence is not attained the iterative process continues in step b).

3. Results

The objectives of the tests reported in this section are to verify the adequacy of the results supplied by the coupling of the boundary layer and Euler codes and also verify the occurrence of convergence. Convergence is an important issue because the literature emphasizes that it may fail if the coupling process is not adequate, or in situations of strong separation and shocks. All tests reported here were done for the RAE 2822 airfoil, which was chosen because there are many experimental and numerical results available for it in the literature.

The inviscid code used in this work can handle two-dimensional problems only as a three-dimensional slice with constant thickness, with no-flux boundary conditions in the upper and lower surface. So the mesh used in these tests was one consisting of triangular prisms and is presented in Fig. 1. The mesh has 11,524 nodes, 10,622 cells and 22,196 ghost cells. The ghost cells are fictitious cells used to set the boundary conditions, see Scalabrin (2002).

The most important entry data for the Euler code are presented in Tab. 1. The CFL number is the Courant, Friedrichs and Levi number and the false diffusion coefficients $\kappa^{(2)}$ and $\kappa^{(4)}$ are defined in Jameson, Schmidt and Turkel (1981).

Table 1 – Input data for the Euler code.

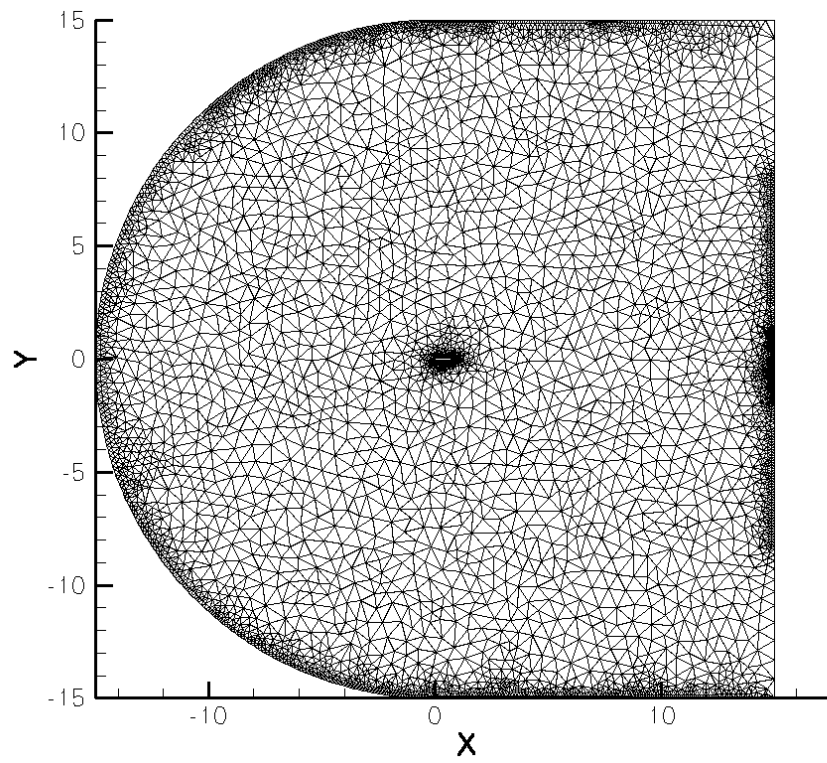
CFL number	0.8
Mach number	0.3 and 0.729
False Diffusion Coefficients	$\kappa^{(2)} = 0.250$ and $\kappa^{(4)} = 0.011718750$

The entry data for used in the boundary layer code are presented in Tab. 2. The code uses a special procedure for the starting the calculation in the stagnation line as described in Cebeci and Bradshaw (1981). The initial thickness of the boundary layer at the stagnation line, η_0 , is defined using the chord, C , and the Reynolds number, Re . The mesh for the boundary layer was created using the nodes of the Euler mesh that were placed in the airfoil's surface.

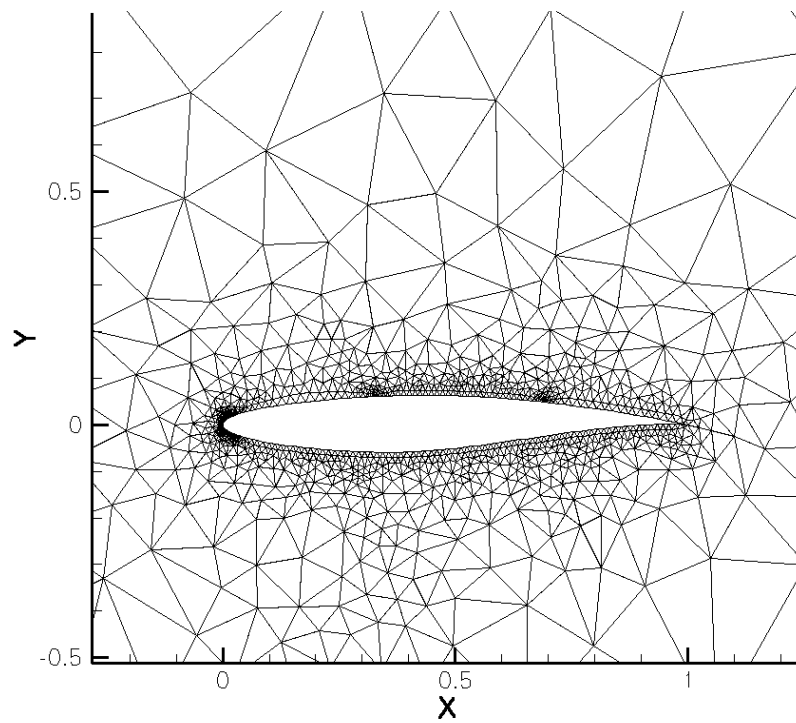
Table 2 – Input data for the boundary layer code.

Reynolds Number:	6.5×10^6
Number of nodes around the airfoil	206
Initial Number of nodes inside the boundary layer	10
Node spacing inside the boundary layer	Geometric progression with $r=1.2$
Dimensionless thickness in the stagnation line	$\eta_0 = y\sqrt{Re}/C = 10$
Point of transition	$x_{tr}/C = 0.03$

In Figure 2 the results for the pressure coefficient, C_p , for $M=0.729$ and $\alpha=2.31^\circ$ are presented. Results are shown for the inviscid (Euler) flow, for the coupled viscous-inviscid flow and the experimental results of Cook, McDonald and Firmin (1979). It can be noticed that, except for the region of supersonic flow ($0 \leq x/C \leq 0.55$ in the upper surface), the use of the viscous-inviscid interaction resulted in an improvement of the results with respect to the experimental results, when compared to the Euler results. In the region of supersonic flow the viscous-inviscid iteration resulted in a reduction of C_p (increase in pressure). So, at a first look, it seems that the viscous-inviscid interaction resulted in a deterioration of the quality of the results in that region.



a) Farfield.



b) Nearfield.

Figure 1 – The mesh used in the RAE 2822 airfoil test case.

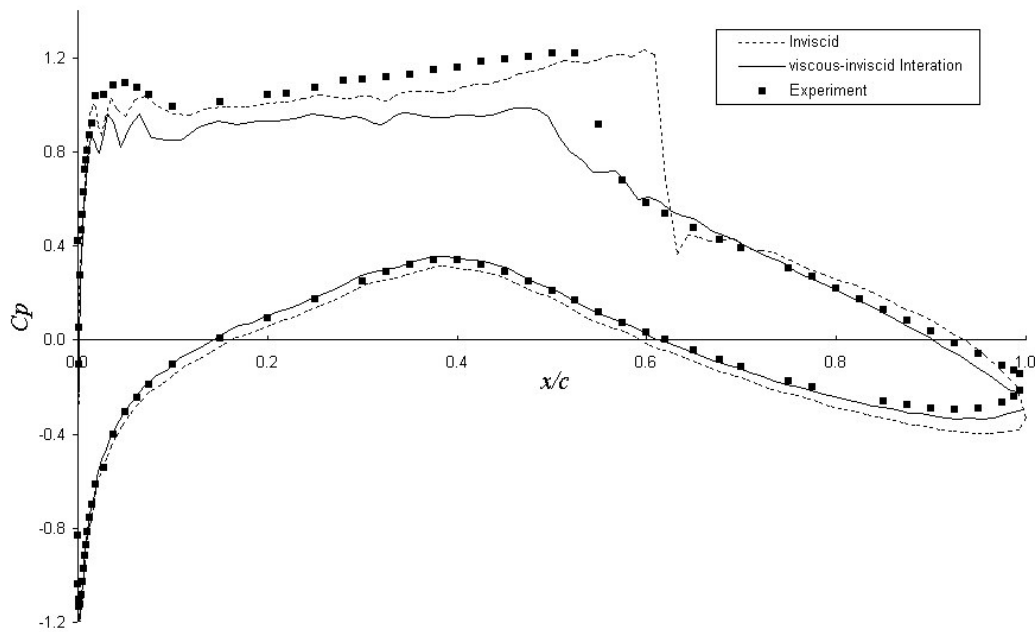


Figure 2 –Pressure coefficient results for the RAE 2822 profile, $M=0.729$ and $\alpha=2.31^\circ$.

Some evidence of the cause of the problem in the supersonic region can be obtained in the work of Coiro et al (1992), that also made computations for the same profile using the Euler formulation alone and using viscous-inviscid iteration. In the results obtained, the C_p values, in the supersonic region, are above the experimental ones and when the viscous-inviscid interaction is introduced, the C_p values decrease, resulting in a good agreement with the experiments. This indicates that the C_p results obtained here were too low, although they seemed adequate, and this resulted in lower C_p values when the boundary layer coupling was done.

Results for the RAE 2822 airfoil obtained by Bruner (1996) with the Euler formulation and Zing *et al.* (1999), using the Navier-Stokes formulation with a turbulence model, show that, when the mesh is not sufficiently refined, a lower C_p value is obtained in the supersonic region precisely like the results obtained here. A qualitative comparison between the mesh used and that of the other authors indicate that the mesh used is coarse and it should be much more refined to obtain a good agreement with the experiments.

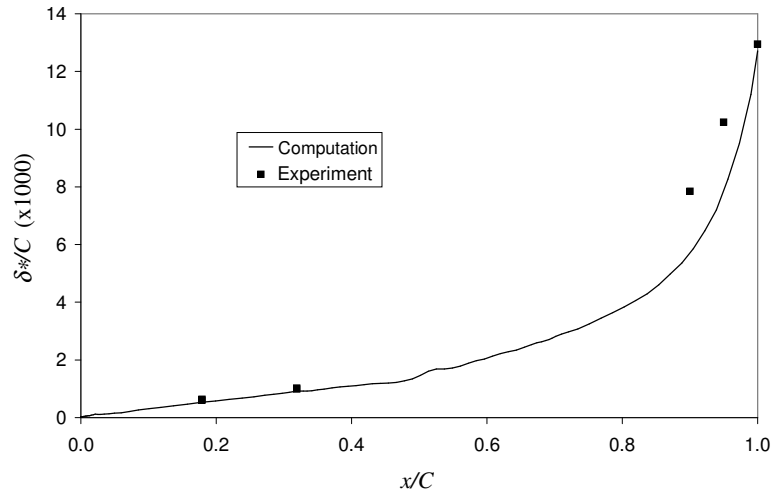
Some numerical experiments with the Euler formulation were done with a more refined mesh and the elevation of C_p values in the supersonic region was noticed. This substantiates the conclusion that the previous mesh was too coarse. Due to the increased CPU times for solution of the refined mesh it wasn't used in any of the other tests.

In Figure 3 results for the displacement thickness, δ^* , momentum thickness, θ , and friction coefficient C_f are presented. It's not clear whether the nondimensionalization for C_f in the experimental work, is based on the far stream velocity or the local velocity outside the boundary layer, u_e . The data presented in Fig. 3 c) use a nondimensionalization with u_e , because it gives a much better agreement with the experimental data.

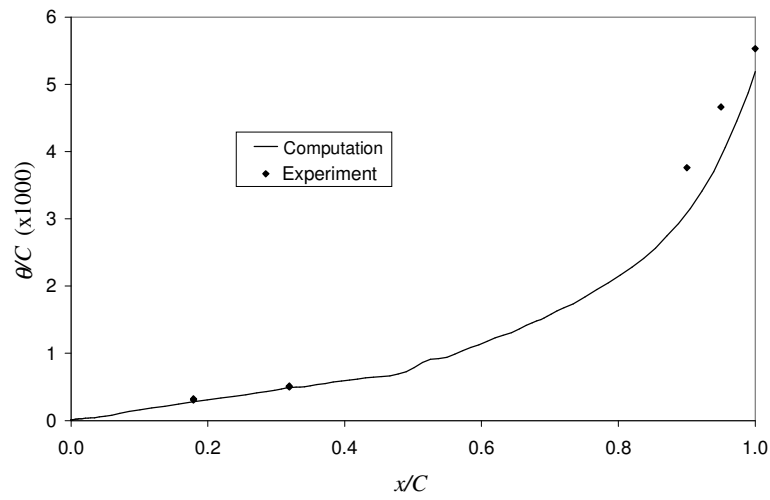
It can be noticed in Fig. 3 that there is a good agreement with the experimental values. The numerical results for the friction coefficient oscillate considerably which is probably due to the fluctuation of the velocities external to the boundary layer.

The number of inviscid iterations between each boundary layer calculation is an important factor for the performance of the iterative procedure. If the number of inviscid iterations is small, the boundary layer program is called many times increasing the computational time. It is also necessary to decrease the relaxation factor, p , because increasing the number of boundary layer calculations will increase the speed in which the transpiration velocity is updated and this can cause divergence. On the other hand, if the number of inviscid iterations is high the entire iterative process will be delayed, because the transpiration velocities are not updated at the necessary pace.

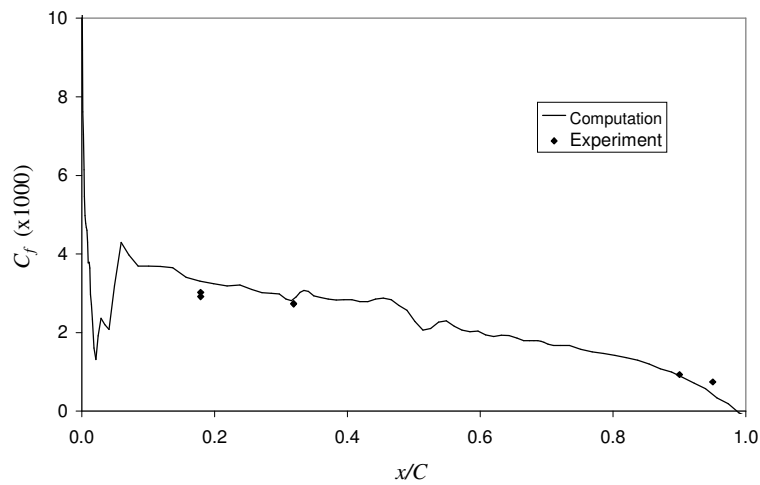
Some experiments were done varying the number of inviscid iterations between each boundary layer calculation and the relaxation factor, to establish optimum values. The experiments indicate that 50 Euler iterations between each boundary layer calculation with a relaxation factor of 0.2 result in the minimum computation time. It's clear that this value will depend on the problem solved, on the parameters of the Euler calculations, on the mesh and other factors and should be used only as a reference for other situations. The increase of CPU time to obtain the iterative viscous-inviscid solution was just 16% when compared to the Euler solution, which is a small price to pay for the increase of precision



a) Displacement thickness.



b) Momentum thickness.



c) Friction coefficient.

Figure 3 – Boundary layer parameters for the RAE 2822 profile, $M=0.729$ and $\alpha=2.3$.

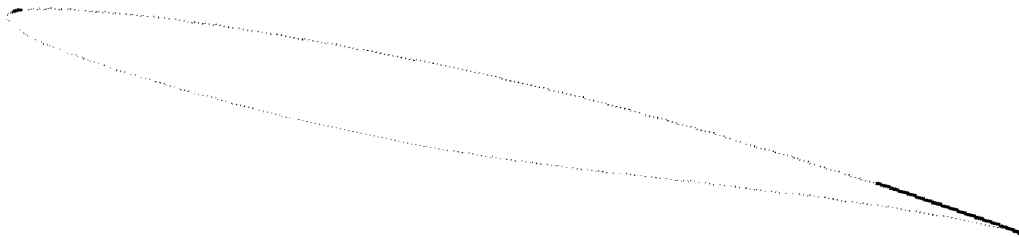
of the viscous-inviscid iteration. This increase in computation time is comparable to the values of 5% cited by Potsdam (1994) and 15% cited by Szmelter (1996), both for a wing and fuselage configuration.

According to the literature, one of the factors that may inhibit convergence of the viscous-inviscid iteration is the occurrence of separation of the boundary layer. It is cited that convergence can be obtained only in cases of mild separation. So, additional tests were made with the objective of verifying the influence of flow separation in convergence. The tests were done also with the RAE 2822 profile at Mach 0.3 and increasing the angle of attack, α , in 2° until convergence problems appear.

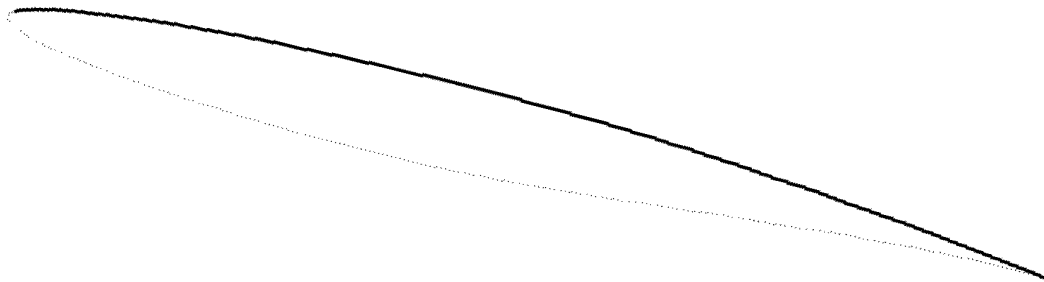
In the tests it was observed that, for $\alpha=6^\circ$, a small separation bubble appears in the upper surface of the leading edge (between $x/c=0.013$ and 0.018), and in the last node of the upper trailing edge. As the angle of attack is increased the extent of the trailing edge separated region increase while the extent of separation bubble at leading edge remains approximately constant. At $\alpha=12^\circ$, the separation bubble at the upper surface extends from $x/c=0.005$ to 0.012 and the trailing edge separation in the upper surface starts at $x/c=0.85$ as presented in Fig. 4 a). At $\alpha=14^\circ$, the separation region increases so that there is one continuous area from $x/c=0.006$ to trailing edge, as presented in Fig. 4 b). For α above 14° , convergence was not attained, probably due to the increased intensity of flow separation and the tendency of an unsteady flow to occur.

It is known that when a separation bubble appears in the leading edge it induces transition to turbulence at that point. Because of this, in the tests, when separation bubbles occurred the transition point was shifted to the same location. It was noticed that, not shifting the point of transition was detrimental for convergence. In some cases convergence was not obtained without shifting the transition point.

Although the viscous-inviscid iteration method used was capable of providing a converged solution with the upper surface of the wing almost completely separated, it must be stressed that the boundary layer solution tend to be less precise than in a flow without separation, because in the regions of reversed flow the boundary layer program disregards the convective term in order to maintain the parabolic character of the equations.



a) Angle of attack $\alpha=12^\circ$.



b) Angle of attack $\alpha=14^\circ$.

Figure 4 - Extent of the separation region (full line) in the RAE 2822 profile.

4. Conclusions

The viscous inviscid iteration technique was successfully applied to the RAE 2822 test case. The comparisons with transonic ($M = 0.729$) experimental results showed good agreement with boundary layer data. For the C_p results, some disagreement was found in regions of the supersonic flow. Results presented in the literature suggest that this disagreement was caused by the coarseness of the mesh. The search for an optimum combination of iteration parameters resulted in a number of 50 inviscid iterations between each boundary layer calculation and a relaxation coefficient of 0.2. Using these parameters the increase of computational time for the viscous-inviscid iteration was just 16% above the required for the Euler flow. The tests done with subsonic flow ($M = 0.3$) and increasing the angle of attack have shown that the coupling technique allows convergence up to a point in which almost all of the upper boundary layer is separated.

5. Acknowledgements

The authors would like to acknowledge the financial support provided by Embraer and FAPESP (grant 00/13768-4).

6. References

- Anderson, D.A., Tannehill, J.C. and Pletcher, R.H., 1984 "Computational Fluid Mechanics and Heat Transfer" Hemisphere Publishing, New York, United States of America, 599 p.
- Anderson, J.D. Jr., 1991, "Fundamentals of Aerodynamics", 2nd ed., McGraw-Hill, New York, United States of America, 772 p.
- Bruner, C.W.S., 1996, "Paralelization of the Euler Equation on Unstructured Grids" PhD Dissertation, Virginia Polytechnic Institute, Blacksburg, United States of America.
- Cebeci, T., 1999, "An Engineering Approach to the Calculation of Aerodynamic Flows", Springer-Verlag, Berlin, Germany, 391 p.
- Cebeci, T., Bradshaw, P., Whitelaw, J.H., 1981, "Engineering Calculation Methods for Turbulent Flow", Academic Press, London, United Kingdom, 331 p.
- Cook, P.H., McDonald, M.A., Firmin, M.C.P., 1979, "Aerofoil RAE 2822 - Pressure Distributions and Boundary Layer and Wake Measurements" AGARD, AR-138. Results also in <http://scholar.lib.vt.edu/ejournals/JFE/data/JFE/DB96-243/d2/f8621>.
- Jameson, A., Schmidt, W., Turkel, E., 1981, "Numerical Solution of the Euler Equations by Finite Volume Methods Using Runge-Kutta Time-Stepping Schemes" Proceedings of the AIAA 14th Plasma and Fluid Dynamics Conference, AIAA paper 81-1259, Palo Alto, United States of America.
- Lock, R.C. and Williams, B.R., 1987, "Viscous-Inviscid Interactions in External Aerodynamics", Progress in Aerospace Science, Vol.24, pp. 51-171.
- Potsdam, M., 1994, "An Unstructured Mesh Euler and Interactive Boundary Layer Method for Complex Configurations", AIAA paper 94-1844.
- Scalabrin, L.C., 2002, "Numerical Simulation of Three-dimensional Flows Over Aerospace Configurations" MsC. Thesis, Instituto Tecnológico de Aeronautica, São José dos Campos, Brazil.
- Schlichting, H., 1979, "Boundary-Layer Theory" 7th ed., McGraw-Hill, New York, United States of America
- Szmelter, J., 1996, "Viscous Coupling Techniques Using Unstructured and Multiblock Meshes" ICAS paper 96-1.7.4.
- Zing, D.W., De Rango, S., Nemec, M. and Pulliam, T.H., 1999, "Comparison of Several Spatial Discretizations for the Navier-Stokes Equations" Proceedings of the 14th AIAA Computational Fluid Dynamics Conference, AIAA paper 99-3260, Norfolk, U.S.A.

7. Responsibility notice

The authors are the only responsible for the printed material included in this paper.